2013 American Control Conference (ACC)
Washington, DC, USA, June 17-19, 2013

Quintessential Phase: A Method of Mitigating Turbulence Effects in Interferometer Measurements of Precision Motion

Eric Johnstone*

Daniel Y. Abramovitch**

***Abstract*— This paper describes a method of mitigating the effect of turbulence in interferometer measurements. In this paper, we will use the example of turbulence disturbing the interferometric estimate of the position of a moving stage, as a 1-D analog of wafer scanning stages used in chip making. The QP method uses a multi-segment detector to detect variations of the drift velocity of the air moving through the interferometer beam, and combines these with a turbulence model to create a set of auxiliary turbulence states. These states are then combined with the states of the moving electromechanical system to form a model of the moving stage in which the turbulence has been removed from the stage position estimate.**

I. Introduction

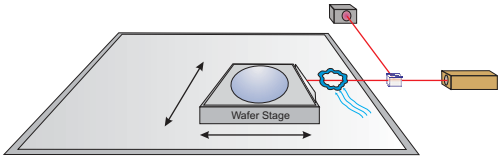

Fig. 1. Conceptual block diagram of wafer stage interferometer (IF) measurement disturbed by turbulence.

Precision interferometers measure distance by measuring the phase difference between an outgoing laser beam and it's return from a reflective surface. When the return signal is combined with the transmitted signal in the interferometer, the resulting phase is related to the distance of the reflected surface from the interferometer. While these measurements are extremely precise, air turbulence can change the density of the air along the beam path, as depicted in Figure 1. This change in air density along the beam path results in an erroneous measure of optical path length which is interpreted as a position error. If the interferometer measurement is used in the feedback loop of the wafer stage controller as shown in Figure 2, then the resulting stage position will mimic the turbulence error.

Interferometers measure the distance to an object by reflecting a coherent light beam off of that object and having the return beam optically interfere with the transmitted beam [1], [2], [3]. The resulting beat signal has a phase relationship with the transmitted beam that is related to the distance to the object. More precisely, it is not the distance that is measured, but the optical path length between the interferometer and the object. In other words, measuring along the z axis, we would like to measure

$$L = \int_0^{Z(t)} dz \tag{1}$$

but instead measure

$$OPL = \int_0^{Z(t)} n(z,y,z)ds \tag{2}$$

where s is the optical path, and $n(z,y,z)$ is the index of refraction along that path.

Environmental effects such as pressure, temperature, and air composition (N_2, O_2, H_2O, etc.) induce a change in the index, $n(x,y,z)$ along the path, s, which is interpreted as an Optical Path Length (OPL) variation.

There have been many attempts to fix the turbulence problem over the years, most of them involving some way of making the optics or the interferometer itself immune to the effects of turbulence.

1) A "weather station" that measures pressure and temperature (which can be implemented as a pressure/temperature sensor or a wavetracker) can help compensate for wavelength variations, but this solution is incomplete because it only accounts for the average temperature and pressure and the bandwidth of these measurements is typically lower than the bandwidth of turbulence.
2) Absorption spectroscopy has been suggested because ... However, this method is complex and requires a predefined assumption of composition the air.
3) Multi-wavelength phase measurement would minimize turbulence effects by measuring the phase at a frequency, f_0, and its first harmonic, $2f_0$. However, this requires the use very short wavelengths and forces a spatial non-coincidence of the index measurement with primary HeNe beam.

The method here is radically different from these in that the turbulence still affects the optical beam, but this effect is detected and modeled. The modeled turbulence is turned into a set of auxiliary measurement states for an Extended Kalman Filter (EKF) [4]. The structure of this paper is as follows: Section II will review the effects of turbulence on interferometry measurements. Section III will describe an optical detector for measuring the change of phase across the wavefront and how these measurements can be incorporated

*Eric Johnstoneis a senior research engineer in the Precision Measuremen Divition of Agilent Technologies, 5301 Stevens Creek Blvd, M/S: 2U, Santa Clara, CA 95051 USA, eric_johnstone@agilent.com

**Daniel Y. Abramovitch is a principal project engineer in the Molecular Imaging Lab at Agilent Laboratories, 5301 Stevens Creek Blvd., M/S: 4L-IC, Santa Clara, CA 95051 USA, danny@agilent.com

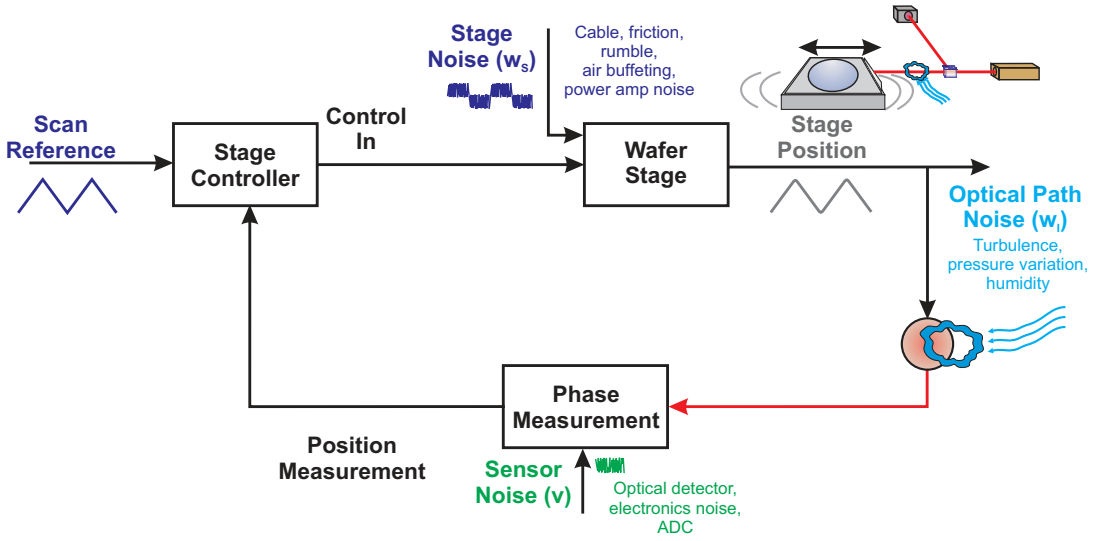

Fig. 2. Conceptual block diagram of wafer stage interferometer (IF) measurement disturbed by turbulence.

into a state space model. Section IV will fold the auxiliary measurement states into an overall EKF model and Section V will describe an experiment done to demonstrate the validity of the method.

II. Interferometry and Turbulence

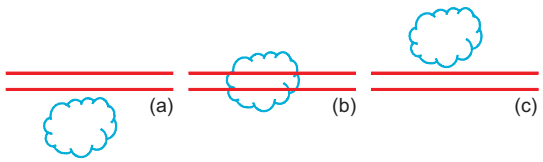

Fig. 3. Turbulence "bubble" crossing interferometer beam.

If one knew $n(x,y,z)$ we could integrate along the path to produce the OPL

$$OPL = \int_{z0}^{z1} n(x,y,z)\sqrt{1+\left(\frac{\partial}{\partial z}x\right)^2+\left(\frac{\partial}{\partial z}y\right)^2}\,dz \quad (3)$$

using the Eikonal Equations:

$$\begin{bmatrix} \frac{\partial}{\partial s}n\left(\frac{\partial}{\partial s}x\right) \\ \frac{\partial}{\partial s}n\left(\frac{\partial}{\partial s}y\right) \end{bmatrix} = \begin{bmatrix} \frac{\partial}{\partial x}n \\ \frac{\partial}{\partial y}n \end{bmatrix}, \quad (4)$$

but we do not known $n(\cdot)$. Consider the image of a turbulence bubble in Figure 3. As time progresses through the sequence (a), (b), (c), we get the undisturbed beam, followed by the beam with the turbulence bubble, followed by the undisturbed beam. The cloud of disturbance did not just appear in thin air like particle creation, it evolved. Furthermore, the dynamics are slow relative to our measurement system, so we can track this evolution. In fact, a relatively simple dynamic model coupled with an estimator removes this from the stage position estimate. To do this, we recast the basic equation for path length by making the index an explicit function of time. The time dependence is slow enough so as not to violate the assumptions of Eikonal Equation derivation(see page 117 of [5]). We can also ignore the square root because we assume that tilts, $\frac{\partial}{\partial z}x$ and $\frac{\partial}{\partial z}d$, due to the index profile are less than 10 rad, which would affect the distance calculation by less than 0.1 ppB. This has been verified experimentally by using a fan blowing with a pressure greater than 2 Pascals across a CLASS 2D laser beam, the deflection is less than 3 μrad, RMS, which is far below the noise floor of the instrument. Furthermore, using Edlén/Ciddor Equations [6], [7], [8], we can related the index of refraction, $n(x,y,z)$ to the air density at a given temperature (P/T). It can be shown that the spectroscopic (dry) component is given by

$$n_S = 1+\chi_s \text{ where} \quad (5)$$

$$\chi_s = 10^{-8}\left(A+\frac{B}{130-\frac{1}{\lambda^2}}+\frac{C}{38.9-\frac{1}{\lambda^2}}\right) \quad (6)$$

which can be modified to account for pressure and temperature as:

$$\chi_{TP} = \frac{D\chi_s P\left(1+7.5*10^{-9}P(4.45-0.0133T_k)\right)}{T_k} \quad (7)$$

$$\chi_{TP} \approx D\chi_s\rho \text{ where } \rho \text{ is the density.} \quad (8)$$

With finite humidity, there is a correction proportional to the partial pressure of water divided by temperature:

$$\chi_{TPw} = E\chi s w\rho_w \text{ so that the index of refraction is} \quad (9)$$

$$n = 1+\chi_{TP}+\chi_{TPw}, \text{ and so we have related } n \text{ to } \rho \text{ so that} \quad (10)$$

$$OPL = \int_0^{L(t)} n(z,y,z,t)dz \quad (11)$$

$$= \int_0^{L(t)} (1 + K\rho(z,y,z,t))\, dz, \quad (12)$$

where the optical path is in the z axis. If we differentiate Equation 11 with time, we get:

$$\frac{\partial}{\partial t}OPL = \frac{d}{dt}L(t) + K\rho(x,y,L,t)\left(\frac{d}{dt}L(t)\right) + K\int_0^{L(t)} \frac{\partial}{\partial t}\rho(x,y,z,t)dz, \quad (13)$$

where the first term is the variation of the actual physical length (what we want to measure), the second term is the length correction due to pressure and temperature variation (which can be corrected with sensors below the interferometer), and the third term is the turbulence correction. This third term is not picked up by the temperature and pressure sensors and so must be observed some other way.

III. Measuring and Modeling the Turbulence

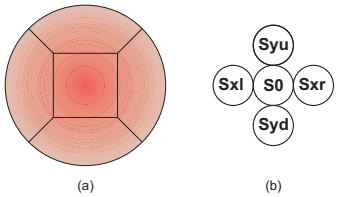

Fig. 4. Multi-segment detector (a) and configuration (b).

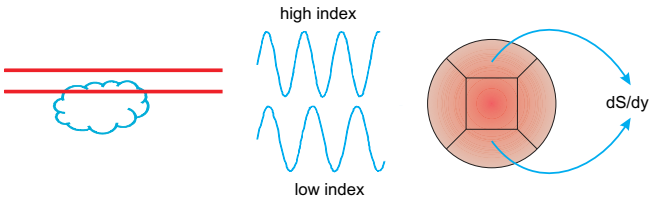

Fig. 5. Turbulence bubble crosses beam lowering the index of refraction and resulting in a phase difference between the lower detector segment and the upper detector segment.

In addition, experiments have shown the effect of sound is negligible so that

$$\nabla \bullet v \approx 0 \quad (14)$$

where v is fluid (drift) velocity in a first order perturbation expansion of the Navier-Stokes/mass-continuity equations. Based on the above assumptions, the rate of turbulence error can be represented by the following equation

$$\frac{d}{dt}\varepsilon(t) = v_x t_x + v_y t_y \quad (15)$$

where $t_x = \frac{\partial}{\partial x}\phi$ and $t_y = \frac{\partial}{\partial y}\phi$. In Equation 15, ε represents turbulence phase as a function of time, v_x and v_y represent x and y components of drift velocity, and ϕ represents the continuous wave function of the electromagnetic field measured by the interferometer system. The parameters v_x and v_y can be estimated from the solutions to:

$$\frac{\partial^2}{\partial x \partial t}\varepsilon(t) = v_x \frac{\partial^2}{\partial x^2}\phi + v_y \frac{\partial^2}{\partial y \partial x}\phi \quad (16)$$

$$\frac{\partial^2}{\partial y \partial t}\varepsilon(t) = v_x \frac{\partial^2}{\partial y \partial x}\phi + v_y \frac{\partial^2}{\partial y^2}\phi \quad (17)$$

First spatial derivatives of the wavefront can be approximated by

$$t_x = \frac{\partial \phi}{\partial x} \approx \frac{S_{xr} - S_{xl}}{2d} \text{ and } t_y = \frac{\partial \phi}{\partial y} \approx \frac{S_{yu} - S_{yd}}{2d}. \quad (18)$$

Similarly, second spatial derivatives can be approximated by:

$$c_x = \frac{\partial^2 \phi}{\partial x^2} \approx \frac{S_{xr} + S_{xl} - 2S0}{d^2} \quad (19)$$

and

$$c_y = \frac{\partial^2 \phi}{\partial y^2} \approx \frac{S_{yu} + S_{yd} - 2S0}{d^2}. \quad (20)$$

When only five detectors are used in a + or a × configuration, the cross terms $\frac{\partial^2}{\partial y \partial x}\phi$ in Equations 16 and 17 are not measurable and are set to 0.

are not measurable

Consider the turbulent part of the optical path length, S:

$$S = K\int_0^L \rho(x,y,z,t)dz. \quad (21)$$

The interferometer will integrate ρ in the z direction, but we can describe the variation of S along the other axes derived from the differential form of a continuity equation for density [9]:

$$\frac{\partial}{\partial t}\rho + \nabla \cdot (\rho \vec{v}) = 0 \quad (22)$$

With a lot of steps which will be omitted here for brevity, Equation 22 can be shown to be equivalent to

$$\frac{\partial}{\partial t}S(x,y,t) + v_{dx}\left(\frac{\partial}{\partial x}S(x,y,t)\right) + v_{dy}\left(\frac{\partial}{\partial y}S(x,y,t)\right) = 0. \quad (23)$$

If we look at the configuration of the multi-segment detector in Figure 4 we find that we can approximate Equation 23 with a difference equation that uses discrete observations of the different detector segments:

$$\frac{\partial}{\partial t}S0 \approx \frac{v_{dx}(Sxl - Sxr)}{2d} + \frac{v_{dy}(Syu - Syd)}{2d} \quad (24)$$

where d represents the distance between the center of the central detector, $S0$, and the center of any of the outlying detectors. Integrating $\frac{\partial}{\partial t}S0$ represents the component of optical path length due to turbulence integrated along the z axis. The first two terms represent the drift velocities, while the last term represents diffusion. The parameter, D, represents a diffusion constant of air, while v_{dx} and v_{dy} represent drift velocities of a disturbance.

If we consider that the central detector, $S0$ contains the optical path length disturbed by turbulence, integrating Equation 24 and subtracting it from $S0$ should give a turbulence

free estimate of the optical path length, which is a turbulence free estimate of distance. The issue, as with any integrator, is that this is not an asymptotically stable process, and thus we need to close the measurement loop using an estimator – in this case an Extended Kalman Filter.

IV. Structure of the Extended Kalman Filter

Equation 24 can be used to construct a state vector for the turbulence states:

$$\begin{bmatrix} \frac{\partial}{\partial t}\varepsilon \\ \varepsilon \\ v_x \\ v_y \end{bmatrix} = \begin{bmatrix} \text{turbulence phase rate} \\ \text{turbulence phase} \\ \text{x component of drift velocity} \\ \text{y component of drift velocity} \end{bmatrix}, \quad (25)$$

With these turbulence states, we can define a measurement vector:

$$\begin{bmatrix} z_1 \\ 0 \\ z_3 \\ z_4 \end{bmatrix} = \begin{bmatrix} \text{central pixel} \\ \text{constraint on rate of change of } \varepsilon \\ \text{rate of change in tilt along x axis} \\ \text{rate of change in tilt along y axis} \end{bmatrix}, \quad (26)$$

but the central pixel measures apparent path length which has components of both actual motion of the electromechanical system and the turbulence disturbance. The innovation vector is defined by:

If we discretize the turbulence states

$$x_{turb}(k) = \begin{bmatrix} \dot{\varepsilon}(k) \\ \varepsilon(k) \\ v_x(k) \\ v_y(k) \end{bmatrix} \quad (27)$$

we can define a state transition for them as

$$\begin{bmatrix} \dot{\varepsilon}_{k+1} \\ \varepsilon_{k+1} \\ v_{x,k+1} \\ v_{y,k+1} \end{bmatrix} = \begin{bmatrix} 0 & 1 & 0 & 0 \\ 1 & T_S & 0 & 0 \\ 0 & 0 & e^{-\frac{T_S}{\tau}} & 0 \\ 0 & 0 & 0 & e^{-\frac{T_S}{\tau}} \end{bmatrix} \begin{bmatrix} \dot{\varepsilon}_k \\ \varepsilon_k \\ v_{x,k} \\ v_{y,k} \end{bmatrix} \quad (28)$$

where there is no input from the controller input to the physical system, $u(k)$. Instead the states are adjusted through feedback from the innovations vector, $\xi(k)$ where

$$\xi_k = \begin{bmatrix} z_{1,k} \\ 0 \\ z_{3,k} \\ z_{4,k} \end{bmatrix} - \begin{bmatrix} D_{mech,D} \\ 0 \\ 0 \\ 0 \end{bmatrix} u_k - \begin{bmatrix} H_{mech,D} & 0 & 1 & 0 & 0 \\ 0 & 1 & 0 & t_x & t_y \\ 0 & 0 & 0 & c_x & 0 \\ 0 & 0 & 0 & 0 & c_y \end{bmatrix} \begin{bmatrix} X_{mech,k} \\ \dot{\varepsilon}_k \\ \varepsilon_k \\ v_{x,k} \\ v_{y,k} \end{bmatrix}. \quad (29)$$

Here we see why the estimator is an Extended Kalman Filter, in that the state output matrix is dependent on the measurements and therefore time varying.

A key realization is that since the central detector measurement is affected by the actual optical path length (OPL) and the turbulence, neither turbulence nor the actual OPL are independently observable from the central pixel measurement alone. Instead, we need both the auxiliary detectors and the physical model of the electromechanical states in order to separate these out. We have not discussed the X_{mech} states, but most of the signal in the central detector comes from the physical motion of these states. Uncertainty in the model effectively leads to a relatively larger process noise model, making the feedback gains from the measurement larger than we might otherwise want.

V. Experimental Results

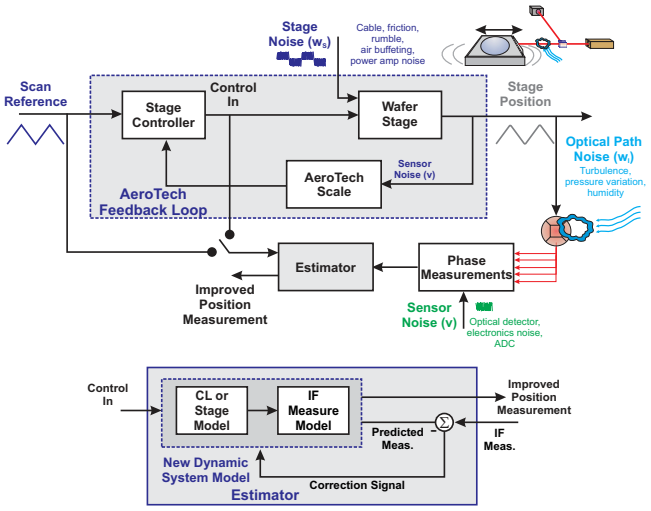

Fig. 6. Conceptual block diagram of wafer stage interferometer (IF) measurement with estimator based correction.

Fig. 7. Laboratory system: Aerotech stage and IF with multi-segment detector.

The algorithm was tested on an Aerotech single axis stage as diagrammed in Figure 6 and shown in Figures 7 and 8. The stage feedback is provided by a digital controller running a PID, sampled at 8 kHz. Turbulence "pulses" were simulated using an air cannon made from a plastic garbage can with an elastic membrane on the back and a small aperture across the front, shown in Figure 8. The pulse strength was modulated by adjusting the tension of the membrane.

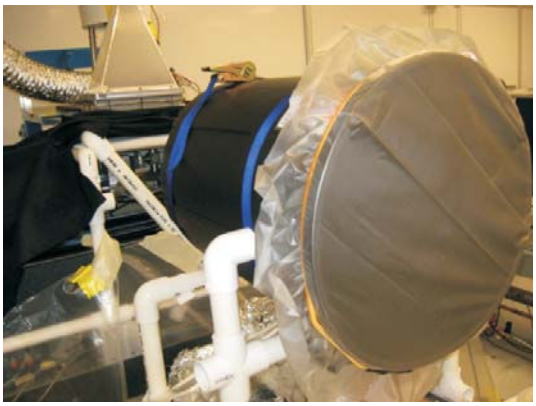

Fig. 8. Laboratory system: air cannon to inject "turbulence" into the system.

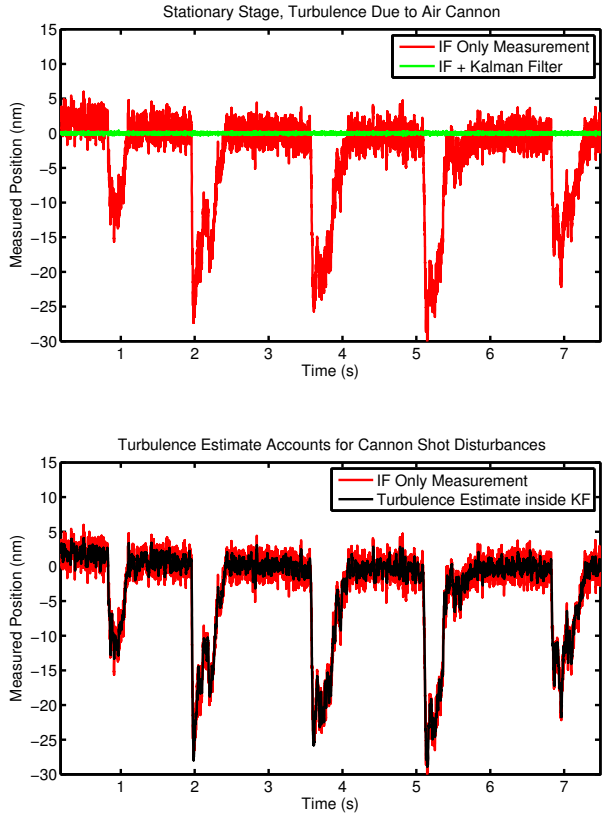

Fig. 9. Experimental results, stationary stage with air cannon shots.

The conventional measurement is from a single segment detector, denoted as the central pixel (CP). This has been consistently shown in red in the data. The EKF estimate is shown in green. The turbulence state estimate is shown in black.

The easiest result to understand is that of Figure 9 in which the stage is stationary. Thus one would expect the central pixel (CP) measurement to be flat, except for the turbulence pulses. We can see from the lower plot that the turbulence model tracks the pulses, so that when they are accounted for in the measurements, the position estimate (in green) shows no disturbance.

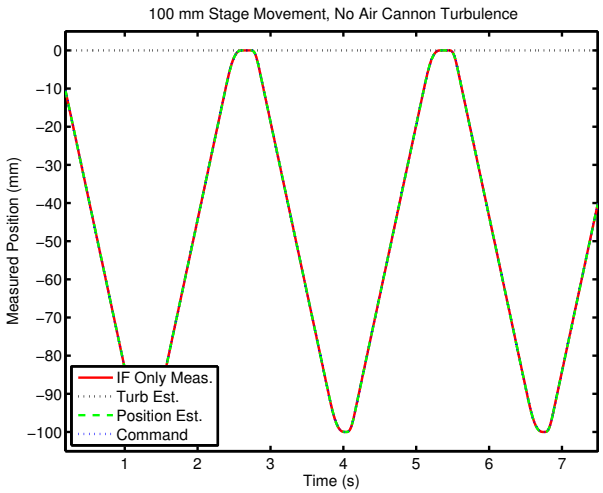

Fig. 10. Experimental results, moving stage no air cannon turbulence.

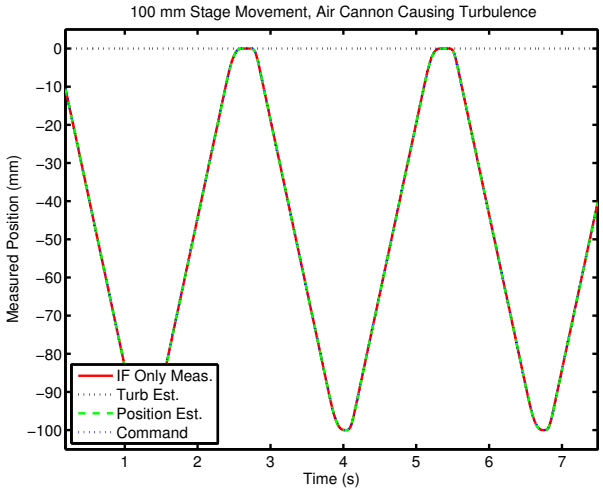

Fig. 11. Experimental results, moving stage with air cannon turbulence.

The litmus test, though, is when the stage is moving. Observing the result becomes more difficult because as can be seen in Figures 10 and 11, the scale of turbulence on a stage moving in a 100 mm triangular sweep is so small as to not be visible. Instead, two similar runs, one without turbulence, and one with are aligned as precisely as possible and differenced, as diagrammed in Figure 12. This removes the common mode motion and reveals a strong difference in the CP plot, which is accounted for in the turbulence states, as shown in Figure 13. However, the difference of the two corrected position estimates (green curve) is negligible, demonstrating that the QP method has desensitized the position measurement from turbulence.

VI. Conclusions

This paper demonstrates a new method for dealing with turbulence in interferometry measurements. The method uses an Extended Kalman Filter with auxiliary measurement states to model the turbulence. Observability of the turbulence states is achieved through the use of a novel multi-segment

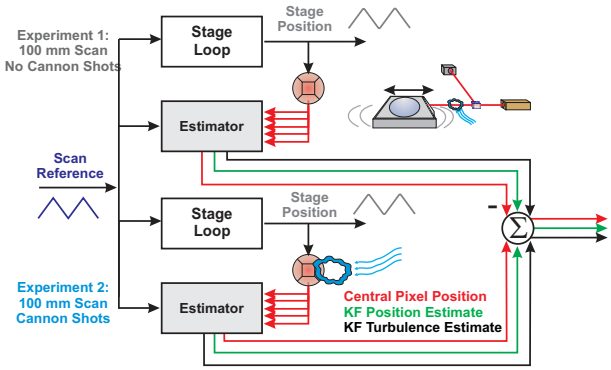

Fig. 12. Experimental setup for moving stage, differencing runs.

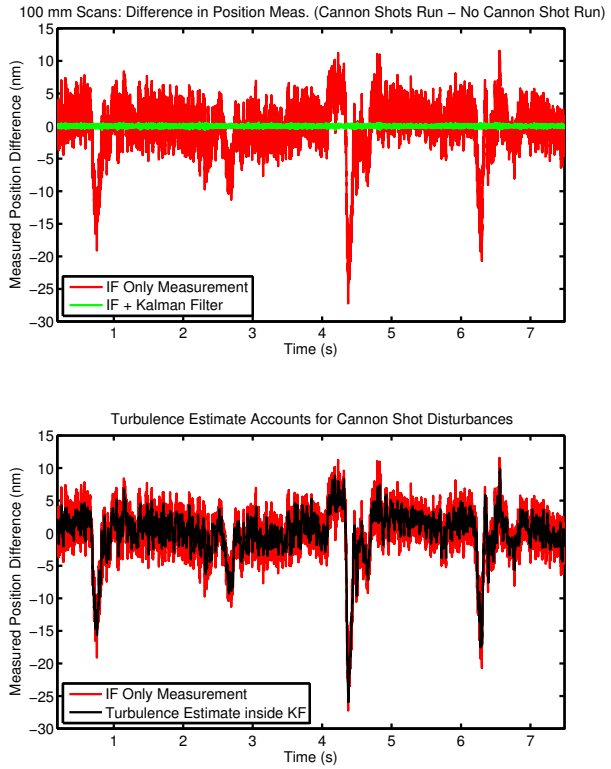

Fig. 13. Experimental results, stage scanning 100 mm, difference of measurements with and without air cannon shots.

detector which allows the detection of the spatial derivatives of the wavefront phase. These derivatives are integrated into the EKF model to form a turbulence state which can then be removed from the central segment measurement of distance plus turbulence. The result is an interferometer measurement that has turbulence effects reduced by a factor of 20.

References

[1] Agilent Technologies, *Agilent Laser and Optics User's Manual, Volume I*, fifth, part number 05517-90086 ed., September 2007.

[2] Agilent Technologies, *Agilent Laser and Optics User's Manual, Volume II*, fifth, part number 05517-90086 ed., July 2007.

[3] E. Hecht and A. Zajac, *Optics*. Addison-Wesley Series in Physics, Reading, MA: Addison-Wesley, 1979.

[4] A. E. Bryson and Y. C. Ho, *Applied Optimal Control*. 1010 Vermont Ave., N. W., Washington, D.C. 20005: Hemisphere Publishing Co., 1975.

[5] M. Born and E. Wolf, *Principles of Optics: Electromagnetic Theory of Propagation, Interference, and Diffraction of Light*. Oxford, England: Pergamon Press, sixth ed., 1980.

[6] B. Edlén, "The refractive index of air," *Metrologia*, vol. 2, pp. 71–80, April 1966.

[7] F. G. Smith, ed., *The Infrared & Electro-Optical Systems Handbook: Volume 2: Atmospheric Propagation and Radiation*. SPIE Optical Engineering Press, 1996.

[8] P. E. Ciddor, "Refractive index of air: New equations for the visible and near infrared," *Applied Optics*, vol. 35, pp. 1566–1573, March 20 1996.

[9] G. K. Batchelor, *An Introduction to Fluid Dynamics*. Cambridge, UK: Cambridge University Press, first ed., 1967.

Appendix

For our standard state model of

$$x(k+1) = \Phi x(k) + \Gamma u(k) \quad (30)$$

$$y(k) = Hx(k) + Du(k) \quad (31)$$

the state matrices would have the form:

$$\Phi = \left[\begin{array}{c|c|c} \text{Electro Mechanical (EM) States} & \text{UI to EM Coupling} & \text{Turb States to EM States} = 0 \\ \hline \text{EM States to UI States} = 0 & \text{UI States} & \text{Turb States to UI States} = 0 \\ \hline \text{EM States to Turb States} = 0 & \text{UI States to Turb States} = 0 & \text{Turbulence States} \end{array}\right], \quad (32)$$

$$H = \left[\begin{array}{c|c|c} \text{EM State to CP Measurement} & \text{UI to CP Measurement} & \text{Turb States to CP Meas.} \\ \hline \text{EM States to Turb Meas.} = 0 & \text{UI States to Turb Meas.} = 0 & \text{Turb States to Turb Meas.} \end{array}\right], \quad (33)$$

$$\Gamma = \left[\begin{array}{c} \text{Controller Output to EM States} \\ \hline \text{Controller Output to UI States} = 0 \\ \hline \text{Controller Output to Turb States} = 0 \end{array}\right], \text{ and } D = \left[\begin{array}{c} \text{Controller Output to CP Measurement} \\ \hline \text{Controller Output to Turb Measurement} = 0 \end{array}\right]. \quad (34)$$

We have allowed for an unmodeled input observer (UI) to be added to this model to account for friction, biases and other unmodeled forces on the stage. Unlike the turbulence states, the unmodeled input state(s) have an affect on the actual position of the stage. On the other hand, our modeling asserts that while the turbulence affects the measurement, its affect on the true stage position is small enough to be ignored. Likewise, the states of the physical system (EM State) do not feed into the turbulence calculations.